3-2024

Light curve and hardness tests for millilensing in GRB 081122A, GRB 081126A, GRB 110517B, and GRB 210812A

Oindabi Mukherjee
Michigan Technological University, omukherj@mtu.edu

Robert J. Nemiroff
Michigan Technological University, nemiroff@mtu.edu

Monthly Notices of the ROYAL ASTRONOMICAL SOCIETY

MNRAS **529,** L83–L87 (2024) https://doi.org/10.1093/mnrasl/slad202
Advance Access publication 2023 December 29

Light curve and hardness tests for millilensing in GRB 081122A, GRB 081126A, GRB 110517B, and GRB 210812A

Oindabi Mukherjee★ and Robert Nemiroff

Department of Physics, Michigan Technological University, 1400, Townsend Dr, Houghton, MI 49931, USA

Accepted 2023 December 26. Received 2023 December 18; in original form 2023 September 30

ABSTRACT

Analyses are given on four recent gravitational millilensing claims on gamma-ray bursts (GRBs): GRB 081122A, GRB 081126A, GRB 110517B, and GRB 210812A. Two tests, a light curve similarity test and a hardness similarity test, compare different temporal sections of a single GRB to see if they are statistically similar. The hardness similarity test shows that the ratio between the second and the first emission episodes in each energy channel differed from the same ratio averaged over all energy channels at above 90 per cent confidence level in GRB 081122A. Additionally, the light curve similarity test applied to GRB 081122A, GRB 081126A, and GRB 110517B separately indicated a high likelihood that the two emission episodes in each GRB were not from the same parent emission episode. This conclusion was reached with confidence levels of 4.8σ for GRB 081122A, 3.08σ for GRB 081126A, and 8.45σ for GRB 110517B. However, these tests did not detect a significant difference between the pulses of GRB 210812A. Consequently, our results suggest that while GRB 210812A could not be conclusively ruled out, the other three GRBs do not show clear evidence of millilensing.

Key words: gravitational lensing: micro – methods: statistical – gamma-ray burst: individual: (GRB 081122A, GRB 081126A, GRB 110517B, and GRB 210812A).

1 INTRODUCTION

The detection of gravitational lensing signatures within the light emitted from Gamma-Ray Bursts (GRBs) offers a unique and promising approach to identifying Compact Objects (COs) scattered throughout the universe, specifically within the mass range of 1 million to 1 billion solar masses. While other sources can be used for detection, GRBs provide a distinct advantage in probing this mass range. This paper aims to review recent claims of gravitational lensing in four individual GRBs.

Press & Gunn (1973) first proposed searching for COs using gravitational lensing. Detecting gravitational lenses from any temporally-resolved source can provide valuable information on the proportion of the universe composed of COs in a specific mass range. Conversely, the lack of detection can constrain the cosmological density and mass values of COs. Therefore, searching for gravitational lensing signatures is crucial for understanding CO dark matter and exploring the universe's properties.

The concept of gravitational lensing in GRBs was first introduced by Paczynski (1987), while Blaes & Webster (1992) proposed using GRBs to detect COs. Earlier attempts to conduct millilensing searches in the Burst and Transient Source Experiment (BATSE) GRBs were made by Nemiroff et al. (2001) and Marani et al. (1999). Ougolnikov (2001) and Li & Li (2014) also conducted similar searches for millilensing in BATSE GRBs, with the former analysing a large sample of 1512 BATSE GRBs. Despite these efforts to detect gravitational lensing signatures in individual GRBs, a clear detection has yet to be made.

Several recent papers have suggested the existence of gravitational millilensing imprints in individual GRBs. Specifically, five papers published in 2021 and 2022 (Paynter, Webster & Thrane 2021, Kalantari et al. 2021, Yang et al. 2021, Wang et al. 2021, and Kalantari, Rahvar & Ibrahim 2022) claim that an early episode of emission is followed by a second episode of emission where both episodes correspond to separate gravitational lens created images of the same parent emission episode.

However, preliminary analyses of GRBs 950830, 090717A, and 200716C by Mukherjee & Nemiroff (2021a), Mukherjee & Nemiroff (2021b), and Mukherjee & Nemiroff (2022) have shown that these GRBs should not be considered as conclusive evidence of gravitational lensing and a more detailed analysis is given by Mukherjee & Nemiroff (2023).

In addition to these three GRBs, four more GRBs have been claimed to be good candidates for millilensing. A paper by Veres et al. (2021) claims that GRB 210812A is gravitationally millilensed, and a separate publication by Lin et al. (2022) suggests the existence of four: GRB 081126A, GRB 090717A, GRB 081122A, and GRB 110517B with varying degrees of confidence.

Mukherjee & Nemiroff (2023) introduced two tests to identify the presence of gravitational lensing: the light curve similarity test and the hardness similarity test. In the simplest gravitational lensing scenario, a compact lens between the observer and the source would create similar images that arrive with different time delays. However, each lens-induced image would be a copy of the same parent GRB, preserving the same light-curve shape and colour-based hardness of

★ E-mail: omukherj@mtu.edu

that parent GRB. However, the total fluence from each image could differ significantly.

The light curve similarity test examines the statistical similarity of light curve shapes between two candidate emission episodes in a single GRB. First, a background level for each GRB is established across individual energy channels using a polynomial fit. With the background set, the process of pulse alignment begins. Here, both $t_{\rm offset}$ and $r_{\rm echo}$ are determined simultaneously, aiming to optimize the resultant χ^2 value. The employed χ^2 formula, essential for gauging light curve resemblance, is adapted from the established works of Cochran (1952) and Press et al. (1992).

The alignment procedure begins by determining the start and end times for each pulse based on the variations in the light curve. The start of the first pulse is identified when the accumulated counts, aggregated over specific time bins, exceed a certain σ threshold above the background fit. When these counts fall below the same σ level, the pulse's end is defined. Based on the premise of gravitational lensing, both pulses, potentially lensed images of the original GRB, are assumed to have the same duration.

When aligning the pulses, it's crucial to factor in shifts in the order of a few microseconds. This granularity is vital for scenarios when the second pulse materializes between two consecutive time bins. Even the slightest misalignment can dramatically skew the χ^2 calculations if not adjusted at the microsecond scale. As such, the recorded counts of the first pulse are modulated in intervals of a few microseconds, iterating through different values of $r_{\rm echo}$, to pinpoint the optimal combination of $t_{\rm offset}$ and $r_{\rm echo}$ that minimizes the χ^2 value.

The challenge in the light curve similarity analysis is that comparing the fainter, extended regions of pulses – often distant from the peak – can suggest similarity through low χ^2 values, even if the core sections are markedly different. This is compounded by the fact that the swift ascent and near-exponential decline characterizing the pulse boundaries render them less unique attributes. With this understanding, the light curve similarity test is designed to compare bins situated close to the pulse apex primarily. We harness the full width at half maximum (FWHM) technique (Jia & Qin 2005) to accomplish this. In this strategy, the bin recording the peak count for the first pulse is pinpointed. Directly after, we identify times accounting for half this peak on either flank of the pulse. With the insights from $t_{\rm offset}$ and the span of the initial pulse, a matching segment in the second pulse is determined.

The hardness similarity test is a technique utilized to analyse the measured colour of each pulse. This test assumes that the gravitational deflection of a photon does not affect its energy, and therefore, the gravitational lensing magnification of a source should be the same at every wavelength, and all gravitational-lens images of the same GRB will have the same hardness.

The test procedure begins by determining the start and end times of pulse 1, which are determined by a designated σ above the background, and the start and end times of pulse 2, which are determined by adding $t_{\rm offset}$ to the start and end times of pulse 1. The counts above the background for both pulses and in all energy bands are calculated using the background fits, pulse start times, and pulse duration. The hardness ratio for each energy channel is then determined by taking the ratio of the summed counts in pulse 2 to those in pulse 1. The errors in these ratios are based on the Poisson noise inherent in the backgrounds and pulses. The formulae used for both the light curve similarity test and the hardness similarity test are detailed in the paper by Mukherjee & Nemiroff (2023).

The remainder of this paper is organized as follows. Section 2 provides a detailed description of the data used, while the results for each GRB are outlined in Section 3. Finally, Section 4 presents the conclusion and summary of the study.

2 DETECTORS AND DATA

The GRBs examined in this study were detected by Fermi's Gamma-ray Burst Monitor (GBM), which comprises 14 detector modules, 12 of which are Sodium Iodide (Na I) detectors and 2 are Bismuth Germanate (BGO) detectors. The Na I detectors cover an energy range of 4 keV–2000 keV, while the BGO detectors cover an energy range of 200 keV–40 MeV.

This study analysed the 2-microsecond Time-Tagged Event (TTE) data, which provided individual counts with high time resolution, recorded over a short time-scale of approximately −30 to 300 s. The TTE data was segmented into eight different energy channels, each with a distinct energy range. These channels were as follows: channel 1 (4.5–11.8 keV), channel 2 (11.8–26.9 keV), channel 3 (26.9–50.4 keV), channel 4 (50.4–101.6 keV), channel 5 (101.6–293.8 keV), channel 6 (293.8–537.8 keV), channel 7 (537.8–983.3 keV), and channel 8 (983.3–2000 keV). Only energy channels that detected a discernible signal above the background were analysed in this study.

3 RESULTS

The detectors and the energy channels that detected signals well above the background were selected for analysing each GRB. After an exploratory analysis, to obtain optimal χ^2 results, a particular time resolution is chosen for all analyses. Table 1 provides information on the detectors, energy channels, and the time resolution used for each GRB.

Light curve similarity test: After the background was fit, optimized values for $t_{\rm offset}$ and $r_{\rm echo}$ were determined, by minimizing χ^2. The FWHM method was used to determine the regions for comparison. It gave the start time (ST) of pulse 1; $t_{\rm lp1}$ and the FWHM duration, $t_{\rm FWHM}$. The start and end times of pulse 2 were obtained by adding $t_{\rm offset}$ to the start and end times of pulse 1. Table 2 provides the values of $t_{\rm offset}$, $r_{\rm echo}$, $t_{\rm lp1}$, $t_{\rm FWHM}$, and σ difference for each GRB.

The compared regions are displayed in Figs 1, 2, 3, and 4. According to the light curve similarity test, the probability that the two pulses were drawn from the same parent pulse is ruled out at greater than 3σ confidence for all GRBs except GRB 210812A.

Lin et al. (2022) claimed that GRB 081122A is gravitationally lensed. This GRB was detected by the Fermi GBM in 2008. From visual inspection of Fig. 1, it can be argued that the two-peak structure of the first pulse is much more clearly defined than the second pulse in 0.256 s time resolution. The χ^2 analysis found that the probability that the two pulses were drawn from the same parent pulse shape was less than approximately 0.00015 per cent, equivalent to above 4.8σ. Considering the 1σ error associated with the bin exhibiting the highest number of counts, there was no variation in the results.

GRB 081126A was claimed to be lensed by Lin et al. (2022). This GRB was also detected by the Fermi GBM in 2008. Fig. 2 shows the two pulses in 0.512 s time resolution. A couple of differences are evident from the visual inspection of these two pulses. Firstly, there are many bins near the peak of the first pulse, whereas there seems to be only one clearly defined peak bin for the second pulse. Secondly, the decay of the second pulse is much slower than the decay of the first pulse. According to the χ^2 results, the two pulses differ in shape at around 3.08σ (or 99.793 per cent). No variation in the results was found considering the 1σ error associated with the bin exhibiting the highest number of counts.

Table 1. The detectors and energy channels used for each GRB.

GRB	Detectors	Energy channels	Time resolution
081122A	n0, n1, n2, n3, n4, n5, n8, n9, and n10	2, 3, 4, 5, and 6	0.256
081126A	n0, n1, n3, and n9	2, 3, 4, 5, and 6	0.512
110517B	n6, n7, and n8	2, 3, 4, and 5	0.256
210812A	n1, n6, n7, n8, n9, n10, and n11	3, 4, 5, and 6	1.024

Table 2. The parameters used for the light curve and hardness similarity tests for each GRB.

GRB	Light curve similarity					Hardness similarity		
	$t_{\rm offset}$	$r_{\rm echo}$	$t_{\rm lp1}$	$t_{\rm FWHM}$	σ difference	$t_{\rm hp1}$	$t_{\rm dur}$	σ difference
081122A	13.816	0.372	0.512	2.56	4.81	−1.28	6.144	1.76
081126A	30.379	0.650	−2.048	4.096	3.08	−2.048	8.192	0.23
110517B	16.612	0.788	0.512	5.12	8.45	−3.328	11.264	0.09
210812A	33.126	0.252	0.0	2.048	0.89	−1.024	9.216	0.45

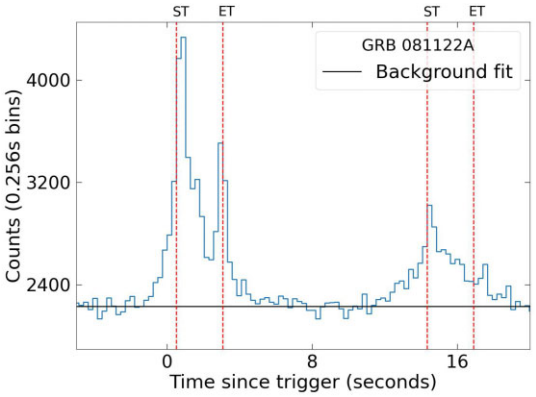

Figure 1. The light curve of GRB 081122A is shown using 0.256 s time bins. The ST and end time (ET) of the comparison regions of the two pulses are shown by vertical dotted lines.

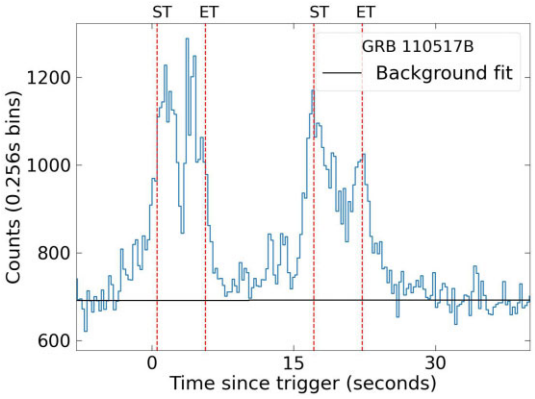

Figure 3. The light curve of GRB 110517B in 0.256 s time bins. The ST and ET of the comparison regions of the two pulses are shown by vertical dotted lines.

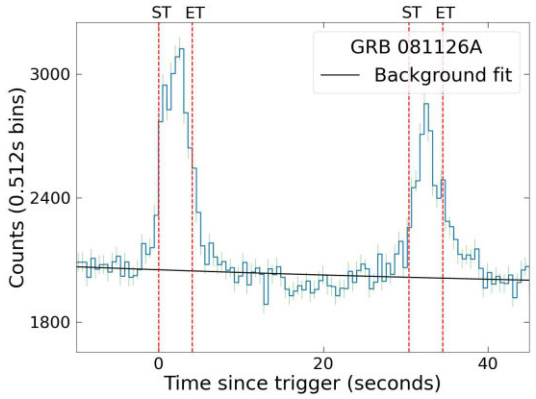

Figure 2. The light curve of GRB 081126A in 1.024 s time bins. The ST and ET of the comparison regions of the two pulses are shown by vertical dotted lines.

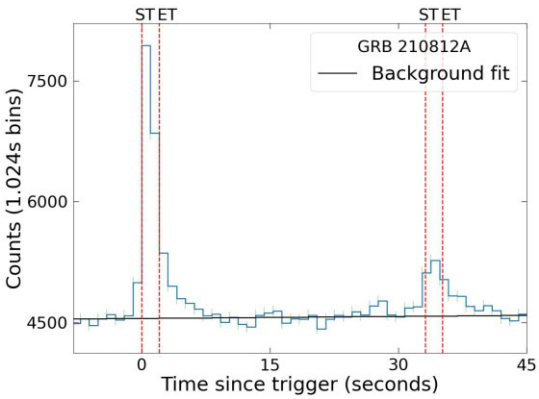

Figure 4. The light curve of GRB 210812A in 1.024 s time bins. The ST and ET of the comparison regions of the two pulses are shown by vertical dotted lines.

The detection of GRB 110517B by Fermi GBM, posited by Lin et al. (2022) to have an echo succeeding the main signal, reveals intriguing distinctions within its pulse structures. An examination of the light-curve plot (Fig. 3) with a 0.256 s time resolution reveals that while both pulses contain two peaks, the intensity of these peaks varies. Specifically, the second peak is more prominent than the first in the initial pulse. However, this order is reversed in the second pulse, where the first peak surpasses the second in brightness. This marked contrast between the two pulses of GRB 110517B stands out at around the $8.45 \pm 0.035\sigma$ confidence level, considering 1σ error in the bin with the maximum counts.

In their study, Veres et al. (2021) proposed that GRB 210812A, detected by Fermi GBM in 2021, contains an echo following the main pulse. Inspecting the 1.024 s light curve (Fig. 4) doesn't immediately

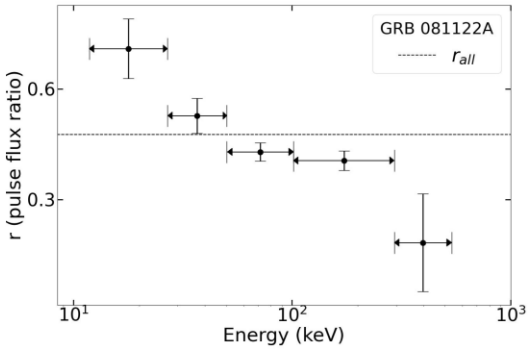

Figure 5. Count ratios between the two main pulses as a function of energy channel for GRB 081122A. The energy channels featured are, from left to right, 2, 3, 4, 5, and 6.

reveal substantial differences between the two pulses. The analysis revealed a divergence at approximately a 0.89σ confidence level, indicating that the test could not find a significant difference between the two pulses. For finer time resolutions, a similar result was obtained for this GRB. However, the second pulse seems broader than the first pulse, so it is likely not millilensed. Still, this GRB remains an intriguing case.

The σ value obtained from χ^2 comparisons between pulses can be affected by binning measured photons at different time resolutions. Higher time resolution, achieved with smaller bin sizes, results in pulses closer to the background and lower comparative σ values. Conversely, lower time resolution, achieved with larger bin sizes, tends to produce higher σ values until the bin duration approaches the duration of the time window being compared. At this point, light-curve shape information is significantly lost. This trend has been consistently observed in all analysed GRBs.

Hardness Similarity Test: The analysis of the start and end times of pulse 1 involved examining the summed counts across all energies. For this test, the ST was defined as when the summed counts in the original time bins first rose above the background fit by over 1σ, located closest to the pulse peak. The pulse was considered to continue until the summed counts dropped below 1σ. The designated ST of Pulse 1 is expressed as $t_{\rm hp1}$. The start and end times of pulse 2 were determined by adding $t_{\rm offset}$ to the start and end time of pulse 1, respectively. Table 2 provides the values of $t_{\rm hp1}$, $t_{\rm dur}$, and σ difference for each GRB.

Figs 5, 6, 7, and 8 displays the r-values between the two pulses for the individual energy channels for GRB 081122A, GRB 081126A, GRB 110517B, and GRB 210812A, respectively. The horizontal line represents the $r_{\rm all}$ value.

The plot for GRB 081122A, Fig. 5 shows the r-values for channels 2, 3, 4, 5, and 6. From a χ^2 test performed to check how different all the r values were from $r_{\rm all}$, it was found that the r values differed from $r_{\rm all}$ at about 1.76σ (or 92.162 per cent). Moreover, the ratio r_2 differs from r_4, r_5, and r_6 by more than 3σ, while the ratio r_3 differs from r_5 and r_6 at about the 2σ level.

Fig. 6 shows the r-values for the energy channels 2, 3, 4, 5, and 6, from left to right for GRB 081126A. The results showed that r_3 differed from r_5 by 1.345σ and r_3 differed from r_5 by 1.796σ, indicating only a marginal difference for GRB 081126A. However, no significant deviation was observed among the r-values from $r_{\rm all}$, suggesting that both pulses had similar energy spectra.

Fig. 7 depicts the r-values for the energy channels 2, 3, 4, and 5, from left to right for GRB 110517B. The analysis found no evidence to reject the similarity of all the r-values from $r_{\rm all}$. All r values were

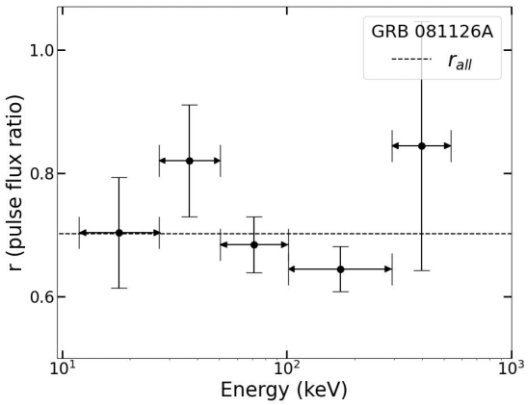

Figure 6. Count ratios between the two pulses as a function of energy channel for GRB 081126A. The energy channels featured are, from left to right, 2, 3, 4, 5, and 6.

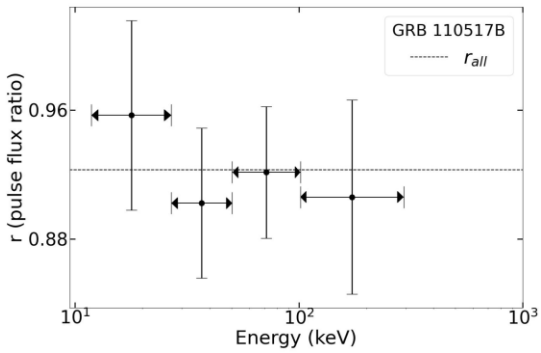

Figure 7. Count ratios between the two pulses as a function of energy channel for GRB 110517B. The energy channels featured are, from left to right, 2, 3, 4, and 5.

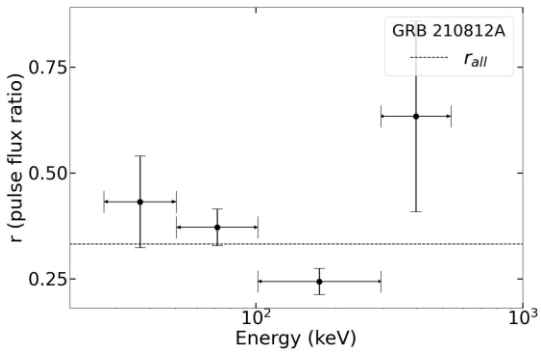

Figure 8. Count ratios between the two pulses as a function of energy channel for GRB 210812A. The energy channels featured are, from left to right, 3, 4, 5, and 6.

statistically consistent with $r_{\rm all}$. Thus, it was concluded that the two pulses have consistent spectra.

The plot for GRB 210812A, Fig. 8 depicts the r-values for the energy channels 3, 4, 5, and 6, from left to right. The analysis found no evidence to reject the similarity of all the r-values from $r_{\rm all}$. The results showed that the r_4 differed from r_5 by 1.768σ, r_3 differed from r_5 by 1.875σ, and r_5 differed from r_6 by 1.313σ. However, it was found that all r values were statistically consistent with $r_{\rm all}$. Thus, it was concluded that the two pulses have consistent spectra.

4 CONCLUSION AND SUMMARY

The primary purpose of this study was to evaluate claims of gravitational millilensing internal to four GRBs: 081122A, 081126A, 110517B, and 210812A. Each GRB had two episodes of emission, here referred to as pulses, that were claimed to be gravitational lens images of the same parent pulses. Two statistical comparison tests were carried out to evaluate the accuracy of these claims: a light curve test comparing the central shapes of each pulse's light curve and a hardness test comparing the overall spectra of the two pulses.

GRB 081122A failed both the light curve and hardness tests because the two pulses in this GRB differed significantly in two different ways. Specifically, for the shape test, it was found that the probability that the two pulses were drawn from the same parent pulse shape was less than approximately 0.00015 per cent, equivalent to above 4.8σ. Furthermore, the hardness test showed that the chance that the spectra of GRB 081122A's two pulses were not measured from the same spectra was about 1.76σ (or 92.162 per cent).

Next, GRB 081126A passed the hardness similarity test but failed the light-curve similarity test, with the light curves of the two pulses differing in shape at above 3.08σ (or 99.793 per cent). While the two pulses of GRB 110517B had statistically similar hardness, their light curves differed from each other markedly – at above the 8.45σ confidence level. Finally, the light curves of the two pulses of GRB 210812A were not found to vary significantly in both light curve and hardness tests.

In conclusion, the analyses of both light curve and hardness tests did not reveal significant variations between the two pulses of GRB 210812A. After thorough testing, this study found no substantial evidence to support the presence of a gravitational lensing effect in GRB 0801122A, GRB 081126A, and GRB 110517B. GRB 210812A, however, presents an intriguing exception.

We thank Michigan Technological University for their general support and reviewer David Palmer for his insightful suggestions.

5 DATA AVAILABILITY

The article's data will be shared with the corresponding author at a reasonable request.

REFERENCES

Blaes O., Webster R., 1992, ApJ, 391, L63
Cochran W. G., 1952, Ann. Math. Stat., 23, 315
Jia L.-W., Qin Y.-P., 2005, ApJ, 631, L25
Kalantari Z., Ibrahim A., Tabar M. R. R., Rahvar S., 2021, ApJ, 922, 77
Kalantari Z., Rahvar S., Ibrahim A., 2022, ApJ, 934, 106
Li C., Li L., 2014, Sci. China: Phys. Mech. Astron., 57, 1592
Lin S.-J. et al., 2022, ApJ, 931, 4
Marani G. F., Nemiroff R. J., Norris J. P., Hurley K., Bonnell J. T., 1999, ApJ, 512, L13
Mukherjee O., Nemiroff R. J., 2021a, Res. Notes AAS, 5, 103
Mukherjee O., Nemiroff R. J., 2021b, Res. Notes AAS, 5, 183
Mukherjee O., Nemiroff R. J., 2022, Res. Notes AAS, 6, 42
Mukherjee O., Nemiroff R., 2023, MNRAS, 527, L132
Nemiroff R. J., Marani G. F., Norris J. P., Bonnell J. T., 2001, Phys. Rev. Lett., 86, 580
Ougolnikov O., 2001, preprint(arXiv preprint astro-ph/0111215)
Paczynski B., 1987, ApJ, 317, L51
Paynter J., Webster R., Thrane E., 2021, Nat. Astron., 5, 560
Press W. H., Gunn J. E., 1973, ApJ, 185, 397
Press W. H., Teukolsky S. A., Flannery B. P., Vetterling W. T., 1992, Numerical recipes in Fortran 77: the art of scientific computing, 2nd edn. Cambridge university press, Cambridge
Veres P., Bhat N., Fraija N., Lesage S., 2021, ApJL, 921, L30
Wang Y., Jiang L.-Y., Li C.-K., Ren J., Tang S.-P., Zhou Z.-M., Liang Y.-F., Fan Y.-Z., 2021, ApJ, 918, L34
Yang X., Lü H.-J., Yuan H.-Y., Rice J., Zhang Z., Zhang B.-B., Liang E.-W., 2021, ApJ, 921, L29

This paper has been typeset from a TEX/LATEX file prepared by the author.